

# Superconductivity in a Two-Orbital Hubbard Model with Electron and Hole Fermi Pockets: Application to Iron Oxypnictide Superconductors

Kazuhiro SANO\* and Yoshiaki ŌNO<sup>1,2</sup>

*Department of Physics Engineering, Mie University, Tsu, Mie 514-8507*

<sup>1</sup>*Department of Physics, Niigata University, Ikarashi, Nishi-ku, Niigata 950-2181*

<sup>2</sup>*Center for Transdisciplinary Research, Niigata University, Ikarashi, Nishi-ku, Niigata 950-2181*

(Received August 27, 2009)

We investigate electronic states of the one-dimensional two-orbital Hubbard model with band splitting by using the exact diagonalization method. The Luttinger liquid parameter  $K_\rho$  is calculated to obtain superconducting (SC) phase diagram as a function of on-site interactions: the intra- and inter-orbital Coulomb  $U$  and  $U'$ , the Hund coupling  $J$  and the pair transfer  $J'$ . In this model, electron and hole Fermi pockets are originated when the Fermi level crosses both upper and lower orbital bands. We find that the system shows two types of SC phases, the SC I for  $U > U'$  and the SC II for  $U < U'$ , in the wide parameter region including both weak and strong correlation regimes. Pairing correlation functions indicate that the most dominant pairing for the SC I (SC II) is the intersite (on-site) intra-orbital spin-singlet with (without) sign reversal of the order parameters between the two Fermi pockets. The result of the SC I is consistent with the sign-reversing  $s$ -wave pairing recently proposed for iron oxypnictide superconductors.

KEYWORDS: iron oxypnictide superconductors, two-orbital Hubbard model, pairing symmetry, exact diagonalization

## 1. Introduction

The recent discovery of the iron oxypnictide superconductors<sup>1-5</sup>) with transition temperatures up to  $T_c \sim 55K$  has stimulated much interest in the relationship between the mechanism of the superconductivity and the orbital degrees of freedom. The first principle calculations have predicted the band structure with the hole Fermi pockets around  $\Gamma$  point and the electron Fermi pockets around  $M$  point.<sup>6-8</sup>) From the weak coupling approaches based on multi-orbital models, the spin-singlet  $s$ -wave pairing is predicted, where order parameter of this pairing changes its sign between the hole and the electron Fermi pockets (the sign-reversing  $s$ -wave pairing).<sup>9-13</sup>) This unconventional  $s$ -wave pairing is expected to emerge due to the effect of the antiferromagnetic spin fluctuations. Since the strong correlation between electrons is considered to play an important role for the superconductivity of the iron oxypnictides as well as that of high- $T_c$  cuprates, non-perturbative and reliable approaches would be required.

As a nonperturbative approach, the exact diagonalization (ED) method has been extensively applied for the Hubbard, the  $d$ - $p$  and the  $t$ - $J$  models.<sup>14</sup>) Although the models are much simplified and mostly limited to one dimension, it has elucidated some important effects of the strong correlation on the superconductivity. Using the ED method, we have studied the one-dimensional (1D) two-orbital Hubbard model in the presence of the band splitting  $\Delta$ . It is found that the superconducting (SC) phase appears in the vicinity of the partially polarized ferromagnetism when the exchange (Hund's rule) coupling  $J$  is larger than a critical value of order of  $\Delta$ .<sup>15</sup>) The result suggests that the spin triplet pairing is expected to emerge due to the effect of the ferromagnetic spin fluctuation. In the case with  $\Delta = 0$ , the spin triplet

superconductivity has also been discussed on the basis of the bosonization<sup>16-18</sup>) and the numerical<sup>19-21</sup>) approaches. The previous works, however, were restricted to the case with single Fermi surface, and the effects of the electron and hole Fermi pockets on the superconductivity have not been discussed there.

In the present paper, we investigate the 1D two-orbital Hubbard model with the electron and hole Fermi pockets, where the Fermi level crosses both upper and lower bands in the presence of a finite band splitting  $\Delta$ . Using the ED method, the Luttinger liquid parameter  $K_\rho$  is calculated to obtain the SC phase diagram as a function of the on-site Coulomb interactions in the wide parameter region including both weak and strong correlation regimes. It would clarify effects of the strong correlation on the superconductivity in the iron oxypnictides. We also calculate various pairing correlation functions and discuss the possible pairing symmetry. Although our model is much simplified and limited to one dimension, we expect that the essence of the superconducting mechanism of the iron oxypnictides can be discussed.

## 2. Model and Formulation

We consider the one-dimensional two-orbital Hubbard model given by the following Hamiltonian:

$$\begin{aligned}
 H = & t \sum_{i,m,\sigma} (c_{i,m,\sigma}^\dagger c_{i+1,m,\sigma} + h.c.) \\
 & + \frac{\Delta}{2} \sum_{i,\sigma} (n_{i,u,\sigma} - n_{i,l,\sigma}) + U \sum_{i,m} n_{i,m,\uparrow} n_{i,m,\downarrow} \\
 & + U' \sum_{i,\sigma} n_{i,u,\sigma} n_{i,l,-\sigma} + (U' - J) \sum_{i,\sigma} n_{i,u,\sigma} n_{i,l,\sigma} \\
 & - J \sum_i (c_{i,u,\uparrow}^\dagger c_{i,u,\downarrow} c_{i,l,\downarrow}^\dagger c_{i,l,\uparrow} + h.c.)
 \end{aligned}$$

\* E-mail address: sano@phen.mie-u.ac.jp

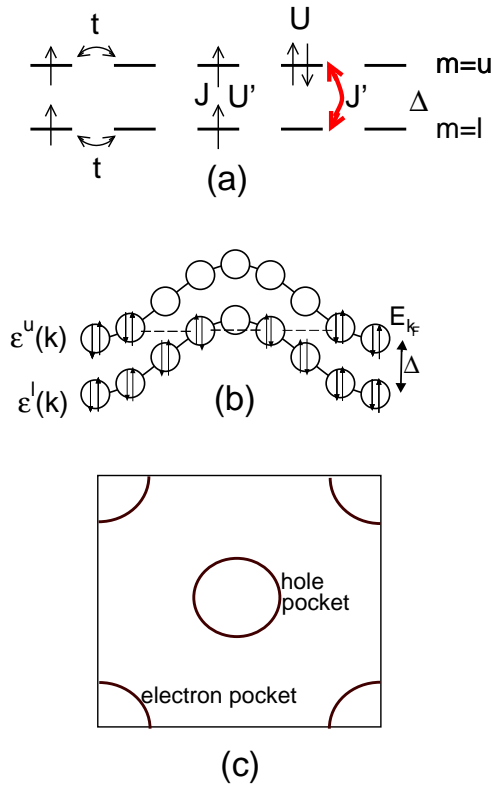


Fig. 1. Schematic diagrams of (a) the model Hamiltonian, (b) the band structure in the noninteracting case, and (c) a corresponding two-dimensional Fermi surface related to our 1D model.

$$- J' \sum_i (c_{i,u,\uparrow}^\dagger c_{i,u,\downarrow}^\dagger c_{i,l,\uparrow} c_{i,l,\downarrow} + h.c.), \quad (1)$$

where  $c_{i,m,\sigma}^\dagger$  stands for the creation operator of an electron with spin  $\sigma$  ( $=\uparrow, \downarrow$ ) and orbital  $m$  ( $=u, l$ ) at site  $i$  and  $n_{i,m,\sigma} = c_{i,m,\sigma}^\dagger c_{i,m,\sigma}$ . Here,  $t$  represents the hopping integral between the same orbitals and we set  $t = 1$  in this study. The interaction parameters  $U$ ,  $U'$ ,  $J$  and  $J'$  stand for the intra- and inter-orbital direct Coulomb interactions, the exchange (Hund's rule) coupling and the pair-transfer, respectively.  $\Delta$  denotes the energy difference between the two atomic orbitals. For simplicity, we impose the relation  $J = J'$ .

The model in eq. (1) is schematically shown in Fig. 1(a). In the noninteracting case ( $U = U' = J = 0$ ), the Hamiltonian eq.(1) yields dispersion relations representing the upper and the lower band energies:  $\epsilon^u(k) = 2t \cos(k) + \frac{\Delta}{2}$ , and  $\epsilon^l(k) = 2t \cos(k) - \frac{\Delta}{2}$ , where  $k$  is the wave vector. This band structure is schematically shown in Fig. 1(b). When the Fermi level,  $E_{k_F}$ , crosses both the upper and lower bands, the system is metallic with the electron and hole Fermi pockets corresponding to a characteristic band structure of FeAs plane in the iron oxypnictides as shown in Fig. 1(c).

We numerically diagonalize the model Hamiltonian up to 6 sites (12 orbitals) and estimate the Luttinger liquid parameter  $K_\rho$  from the ground state energy of finite size systems using the standard Lanczos algorithm.<sup>14)</sup> To reduce the finite size effect, we impose the boundary condition (the periodic or the antiperiodic one) on upper and lower orbitals independently and chose the both

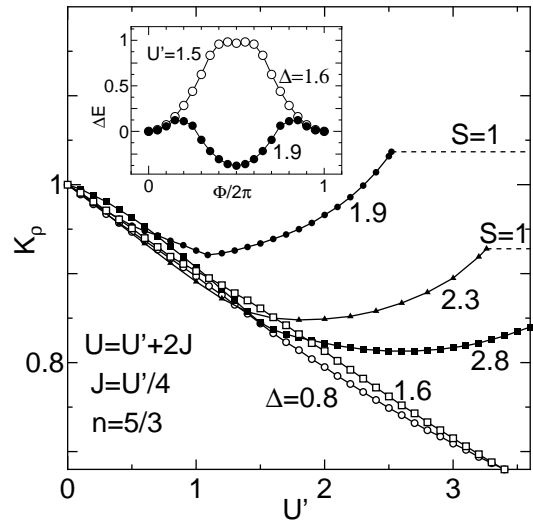


Fig. 2.  $K_\rho$  as a function of  $U'$  ( $=4J$ ) for  $n = 5/3$  (10 electrons/6 sites) at  $\Delta = 0.8, 1.6, 1.9, 2.3$  and  $2.8$ . The singlet ground state changes into the partially polarized ferromagnetic ( $S=1$ ) state at  $U' \simeq 2.5, 3.2$  and  $4.1$  for  $\Delta = 1.9, 2.3$  and  $2.8$ , respectively. Inset shows the energy difference  $E_0(\phi) - E_0(0)$  as a function of an external flux  $\phi$  for  $n = 2/3$  (6 electrons/9 sites) at  $\Delta = 1.2$ .

boundary conditions to minimize the value of  $|K_\rho^0 - 1|$ , where  $K_\rho^0$  represents  $K_\rho$  of the finite size system in the non-interacting case. Typical deviation of  $K_\rho$  from unity becomes about  $\sim 0.1$  for a 6 sites system. For simplicity, we will redefine  $K_\rho$  as a renormalize value calculated by  $K_\rho/K_\rho^0$ , hereafter.

On the basis of the Tomonaga-Luttinger liquid theory,<sup>22-26)</sup> various types of correlation functions are determined by a single parameter  $K_\rho$  in the model which is isotropic in spin space. For single-band model with two Fermi points,  $\pm k_F$ , the SC correlation function decays as  $\sim r^{-(1+\frac{1}{K_\rho})}$ , while the CDW and SDW correlation functions decay as  $\sim \cos(2k_F r) r^{-(1+K_\rho)}$ . Thus, the SC correlation is dominant for  $K_\rho > 1$ , while the CDW or SDW correlation is dominant for  $K_\rho < 1$ . On the other hand, for two-band model with four Fermi points,  $\pm k_{F1}$  and  $\pm k_{F2}$ , the low-energy excitations are given by a single gapless charge mode with a gapped spin mode.<sup>25-27)</sup> In this case, the SC and the CDW correlations decay as  $\sim r^{-\frac{1}{2K_\rho}}$  and  $\sim \cos[2(k_{F2} - k_{F1})r] r^{-2K_\rho}$ , respectively, while the SDW correlation decays exponentially. Hence, the SC correlation is dominant for  $K_\rho > 0.5$ , while, the CDW correlation is dominant for  $K_\rho < 0.5$ . In either case, the SC correlation increases with the exponent  $K_\rho$ , and then  $K_\rho$  is regarded as a good indicator of the superconductivity. As the non-interacting value of  $K_\rho$  is always unity, we assume that the condition of  $K_\rho > 1$  for our model is corresponding to the superconducting state which is realized in oxypnictide superconductors.

### 3. Phase diagram

Figure 2 shows the value of  $K_\rho$  as a function of  $U'$  for several values of  $\Delta$  at the electron density  $n = 5/3$  (10 electrons/6 sites), where we set  $J = U'/4$  with  $U = U' + 2J$ . When  $U'$  increases,  $K_\rho$  decreases for a

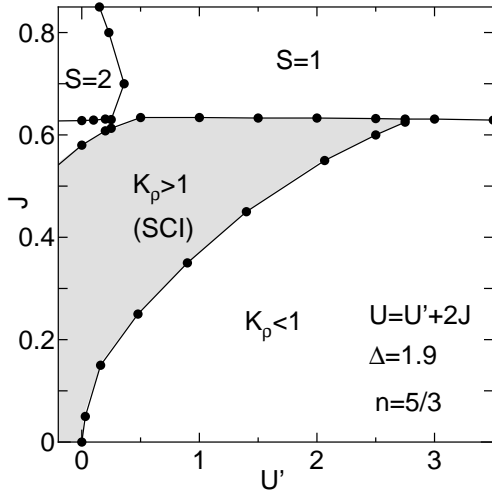


Fig. 3. Phase diagram of the ground state with the value of  $K_\rho$  on the  $U' - J$  parameter plane with  $U = U' + 2J$  for  $n = 5/3$  (10 electrons/6 sites) at  $\Delta = 1.9$ .

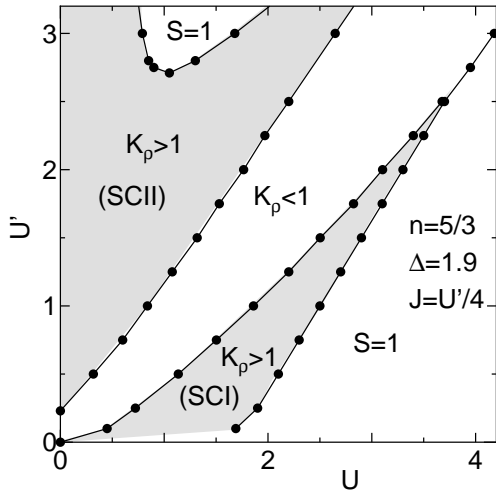


Fig. 4. Phase diagram of the ground state with the value of  $K_\rho$  on the  $U - U'$  parameter plane with  $J = U'/4$  for  $n = 5/3$  (10 electrons/6 sites) at  $\Delta = 1.9$ .

small  $U'$ , while it increases for a large  $U'$  in the case with  $\Delta \geq 1.9$ , and then becomes larger than unity for  $U' > 2.3$  with  $\Delta = 1.9$ . When  $J (= U'/4)$  is larger than a certain critical value, the ground state changes into the partially polarized ferromagnetic state with total spin  $S = 1$  from the singlet state with  $S = 0$ . We find that the superconductivity is most enhanced in the vicinity of the partially polarized ferromagnetic state. To confirm the superconductivity, we calculate the energy difference of the ground state  $E_0(\phi) - E_0(0)$  as a function of an external flux  $\phi$ . As shown in the inset of Fig. 2, anomalous flux quantization is clearly observed for  $\Delta = 1.9$  while not for  $\Delta = 0.8$ .

In Fig.3, we show the phase diagram of the ground state on the  $U' - J$  parameter plane under the condition of  $U = U' + 2J$  for  $n = 5/3$  (10 electrons/6 sites) at  $\Delta = 1.9$ . It contains the singlet state with  $S = 0$  together with partially polarized ferromagnetic states with

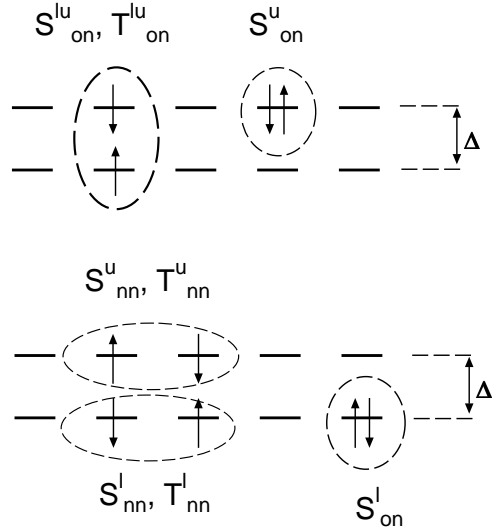


Fig. 5. Schematic diagrams of various types of superconducting pairing symmetries;  $S_{\text{on}}^l, S_{\text{on}}^u, S_{\text{nn}}^l, S_{\text{nn}}^u, S_{\text{on}}^u$  with spin singlet pairings and  $T_{\text{nn}}^l, T_{\text{nn}}^u, T_{\text{on}}^u$  with spin triplet pairings.

$S = 1$  and  $S = 2$ . The singlet state with  $K_\rho > 1$ , where we call it the *SC* phase, appears near the partially polarized ferromagnetic region at  $J \gtrsim U'$ . It extends from the attractive region ( $U' < 0$ ) to the realistic parameter region with  $J \sim U'/4 > 0$  which is expected to correspond to the case with iron oxypnictides.<sup>8)</sup> We have confirmed that similar phase diagrams are obtained also for  $\Delta = 2.3$  and 2.6.

Figure 4 shows the phase diagram of the ground state on the  $U - U'$  plane under the condition of  $J = U'/4$  for  $n = 5/3$  (10 electrons/6 sites) at  $\Delta = 1.9$ . We observe two types of SC phases with  $K_\rho > 1$ , the SC I for  $U > U'$  and the SC II for  $U < U'$ , in the wide parameter region including both weak and strong correlation regimes. We note that the SC I corresponds to the SC phase shown in Fig.3 and belongs to the realistic parameter region mentioned before.

#### 4. Pairing correlation

To examine the nature of these SC phases, we calculate SC pairing correlation functions for various types of pairing symmetries schematically shown in Fig. 5. Explicit forms of the SC pairing correlation functions  $C(r)$  are given by

$$\begin{aligned}
 S_{\text{on}}^l(r) &= \frac{1}{N} \sum_i \langle c_{i,l,\uparrow}^\dagger c_{i,l,\downarrow}^\dagger c_{i+r,l,\downarrow} c_{i+r,l,\uparrow} \rangle, \\
 S_{\text{on}}^u(r) &= \frac{1}{N} \sum_i \langle c_{i,u,\uparrow}^\dagger c_{i,u,\downarrow}^\dagger c_{i+r,u,\downarrow} c_{i+r,u,\uparrow} \rangle, \\
 S_{\text{nn}}^l(r) &= \frac{1}{2N} \sum_i \langle (c_{i,l,\uparrow}^\dagger c_{i+1,l,\downarrow}^\dagger - c_{i,l,\downarrow}^\dagger c_{i+1,l,\uparrow}^\dagger) \\
 &\quad \times (c_{i+r+1,\downarrow} c_{i+r,l,\uparrow} - c_{i+r+1,\uparrow} c_{i+r,l,\downarrow}) \rangle, \\
 S_{\text{nn}}^u(r) &= \frac{1}{2N} \sum_i \langle (c_{i,u,\uparrow}^\dagger c_{i+1,u,\downarrow}^\dagger - c_{i,u,\downarrow}^\dagger c_{i+1,u,\uparrow}^\dagger) \\
 &\quad \times (c_{i+r+1,u,\downarrow} c_{i+r,u,\uparrow} - c_{i+r+1,u,\uparrow} c_{i+r,u,\downarrow}) \rangle,
 \end{aligned}$$

$$\begin{aligned}
S_{\text{on}}^{\text{lu}}(r) &= \frac{1}{2N_u} \sum_i \langle (c_{i,l,\uparrow}^\dagger c_{i,u,\downarrow}^\dagger - c_{i,l,\downarrow}^\dagger c_{i,u,\uparrow}^\dagger) \\
&\quad \times (c_{i+r,u,\downarrow} c_{i+r,l,\uparrow} - c_{i+r,u,\uparrow} c_{i+r,l,\downarrow}) \rangle, \\
T_{\text{nn}}^{\text{l}}(r) &= \frac{1}{2N_u} \sum_i \langle (c_{i,l,\uparrow}^\dagger c_{i+1,l,\downarrow}^\dagger + c_{i,l,\downarrow}^\dagger c_{i+1,l,\uparrow}^\dagger) \\
&\quad \times (c_{i+r+1,\downarrow} c_{i+r,l,\uparrow} + c_{i+r+1,\uparrow} c_{i+r,l,\downarrow}) \rangle, \\
T_{\text{nn}}^{\text{u}}(r) &= \frac{1}{2N_u} \sum_i \langle (c_{i,u,\uparrow}^\dagger c_{i+1,u,\downarrow}^\dagger + c_{i,u,\downarrow}^\dagger c_{i+1,u,\uparrow}^\dagger) \\
&\quad \times (c_{i+r+1,u,\downarrow} c_{i+r,u,\uparrow} + c_{i+r+1,u,\uparrow} c_{i+r,u,\downarrow}) \rangle, \\
T_{\text{on}}^{\text{lu}}(r) &= \frac{1}{2N_u} \sum_i \langle (c_{i,l,\uparrow}^\dagger c_{i,u,\downarrow}^\dagger + c_{i,l,\downarrow}^\dagger c_{i,u,\uparrow}^\dagger) \\
&\quad \times (c_{i+r,u,\downarrow} c_{i+r,l,\uparrow} + c_{i+r,u,\uparrow} c_{i+r,l,\downarrow}) \rangle,
\end{aligned}$$

where  $S_{\text{on}}^{\text{l}}(r)$ ,  $S_{\text{on}}^{\text{u}}(r)$ ,  $S_{\text{nn}}^{\text{l}}(r)$ ,  $S_{\text{nn}}^{\text{u}}(r)$  and  $S_{\text{on}}^{\text{lu}}(r)$  denote the singlet pairing correlation functions on the same site in the lower orbital, on the same site in the upper orbital, between the nearest neighbor sites in the lower orbital, between the nearest neighbor sites in the upper orbital, between lower and upper orbitals on the same site, respectively. Further,  $T_{\text{nn}}^{\text{l}}(r)$ ,  $T_{\text{nn}}^{\text{u}}(r)$  and  $T_{\text{on}}^{\text{lu}}(r)$  are the triplet pairing correlation functions between the nearest neighbor sites in the lower orbital, between the nearest neighbor sites in the upper orbital and between lower and upper orbitals on the same site, respectively.

In Fig.6, we show the absolute values of various types of SC paring correlation functions  $|C(r)|$  for  $n = 5/3$  (10 electrons/6 sites) at  $\Delta = 1.9$ ,  $U' = 4J = 1.0$  and  $U = -0.4$ . Here the electronic state of the system belongs to the SC II phase, although the phase diagram for  $U < 0$  is not explicitly shown in Fig.4. We note that  $|T_{\text{nn}}^{\text{u}}(r)| < 10^{-4}$  and  $S_{\text{on}}^{\text{lu}}(r = 3) = T_{\text{on}}^{\text{lu}}(r = 3) = 0$ , which are not shown in Fig.6. We find that  $S_{\text{on}}^{\text{u}}(r)$  and  $S_{\text{nn}}^{\text{u}}(r)$  decay very slowly as functions of  $r$  and  $|S_{\text{on}}^{\text{u}}(r = 3)|$  is the largest among the various  $|C(r = 3)|$ . Therefore, the relevant pairing symmetry for the SC II phase seems to be the spin singlet pairing in the upper orbital band and mainly consists of 'on-site' pairing. It is considered that such pairing for attractive region with  $U < 0$  is due to the intra-orbital attraction  $U$ . On the other hand, for repulsive region with  $U' > U > 0$ , the paring may be due to the charge fluctuation which is enhanced by the large inter-orbital repulsion  $U'$  as similar to the case of the  $d$ - $p$  model in the presence of the inter-orbital repulsion  $U_{pd}$ .<sup>28)</sup>

Next we discuss the superconductivity in the SC I phase including realistic parameter region as mentioned before. Fig.7 indicates the absolute values of various types of SC paring correlation functions  $|C(r)|$  for  $n = 5/3$  (10 electrons/6 sites) at  $\Delta = 1.9$ ,  $U' = 4J = 1.0$  and  $U = 2.4$ , where the system belongs to the SC I phase as shown in Fig.4. Here,  $|T_{\text{nn}}^{\text{l}}(r)|$ ,  $|S_{\text{on}}^{\text{lu}}(r = 3)|$ , and  $|T_{\text{on}}^{\text{lu}}(r = 3)|$  are not shown, because those correlation functions are very small or zero as well as the case of Fig.6. We find that  $|S_{\text{on}}^{\text{u}}(r)|$  is considerably suppressed as compared to  $|S_{\text{nn}}^{\text{u}}(r)|$  in contrast to the case with the SC II phase. Further,  $|S_{\text{nn}}^{\text{l}}(r)|$  increases with increasing  $r$  except for  $r = 2$ . Therefore, the relevant pairing sym-

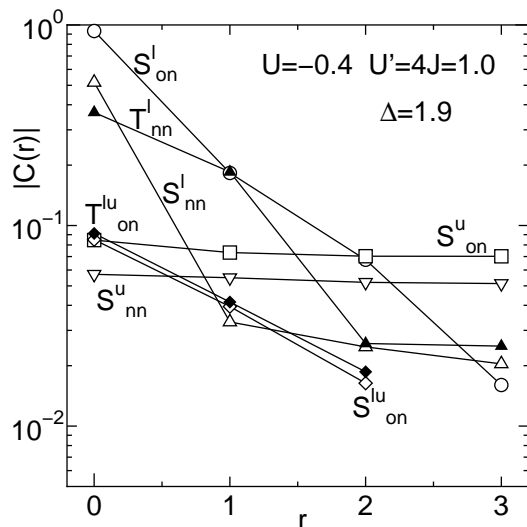


Fig. 6. The the absolute values of various types of SC paring correlation functions  $|C(r)|$  as functions of  $r$  for  $n=5/3$  (10 electrons/6 sites) at  $\Delta = 1.9$ ,  $U' (= 4J) = 1.0$  and  $U = -0.4$ , corresponding to the SC II phase.

metry for the SC I phase seems to be an extended spin singlet pairing and mainly consists of nearest-neighbor site pairing.

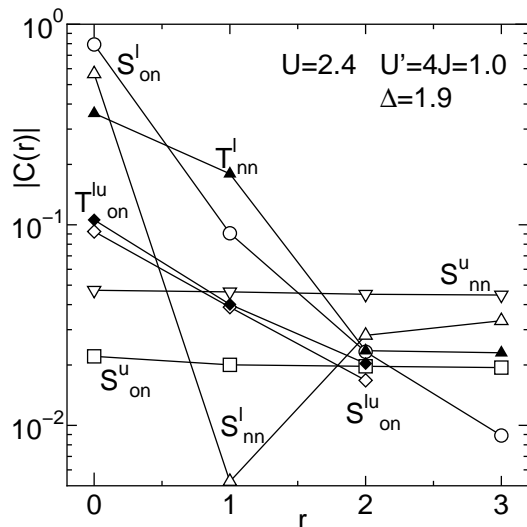


Fig. 7. The absolute values of various types of SC paring correlation functions  $|C(r)|$  as functions of  $r$  for  $n=5/3$  (10 electrons/6 sites) at  $\Delta = 1.9$ ,  $U' (= 4J) = 1.0$  and  $U = 2.4$ , corresponding to the SC I phase.

Recently, weak coupling approaches such as RPA and perturbation expansions have claimed that the sign-reversing  $s$ -wave ( $s_{\pm}$ -wave) pairing is realized in the iron oxypnictide superconductors.<sup>9-13)</sup> The order parameter of that paring is considered to change its sign between the hole and the electron Fermi pockets. To compare our result with the weak coupling result, we examine the SC paring correlation function between the *lower* and *upper* orbitals, such as

$$S_{\text{nn}}^{\text{l-u}}(r) = \frac{1}{2N} \sum_i \langle \Delta_{\text{nn}}^{\text{l}}(i)^\dagger \Delta_{\text{nn}}^{\text{u}}(i+r) \rangle$$

with

$$\Delta_{nn}^m(i)^\dagger = c_{i,m,\uparrow}^\dagger c_{i+1,m,\downarrow}^\dagger - c_{i,m,\downarrow}^\dagger c_{i+1,m,\uparrow}^\dagger \quad (m = l, u).$$

We also define  $T_{nn}^{l-u}(r)$  as well as  $S_{nn}^{l-u}(r)$  in the above equation.

When the  $s_{\pm}$ -wave pairing is dominate, the values of the inter-orbital SC pairing correlation function are expected to be negative, since the Fermi surface of the lower (upper) orbital band in our model corresponds to the hole (electron) Fermi pocket as shown in Fig.1(b). In Fig.8, we show the inter-orbital pairing correlation functions  $S_{nn}^{l-u}(r)$  and  $T_{nn}^{l-u}(r)$ (see also inset) for the same parameters in Fig.4 corresponding to the SC I phase. We see that the values of  $T_{nn}^{l-u}(r)$  are positive and very small, while the values of  $S_{nn}^{l-u}(r)$  are negative except for  $r = 3$  and not so small. The result suggests that the relevant pairing symmetry of the SC I phase is the spin-singlet  $s_{\pm}$ -wave pairing and agrees with the result from the weak coupling approaches. Therefore, we expect that the  $s_{\pm}$ -wave pairing proposed by the weak coupling approaches is realized in the wide parameter region including both weak and strong correlation regimes.

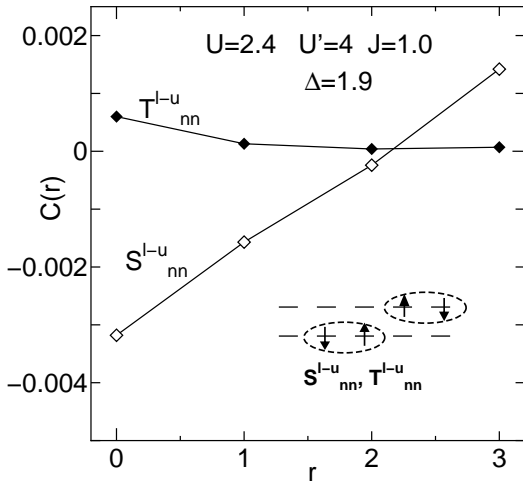


Fig. 8. The pairing correlation functions  $S_{nn}^{l-u}(r)$ , and  $T_{nn}^{l-u}(r)$ , respectively. Here we show the absolute value of the correlation functions at  $U = 2.4$  and  $\Delta = 1.9$ ,  $U' (= 4J) = 1.0$  for  $n=5/3$  (10 electrons/6 sites). Inset shows a schematic diagram of pairing symmetries;  $S_{nn}^{l-u}(r)$ , and  $T_{nn}^{l-u}(r)$ .

## 5. Summary and Discussion

We have investigated the superconductivity of the one-dimensional two-orbital Hubbard model in the case of electron and hole Fermi pockets corresponding to a characteristic band structure of the iron oxypnictide superconductors. To obtain reliable results including for strong correlation regime, we have used the exact diagonalization method and calculated the critical exponent  $K_\rho$  based on the Luttinger liquid theory. It has been found that the system shows two types of SC phases, the SC I for  $U > U'$  and the SC II for  $U < U'$ , in the wide parameter region including both weak and strong correlation regimes.

We have also calculated various types of SC pairing

correlation functions in realistic parameter region of the iron oxypnictides. It indicates that the most dominant pairing for the SC I phase is the intersite intra-orbital spin-singlet with sign reversal of the order parameters between the two Fermi pockets. The result is consistent with the sign-reversing  $s$ -wave pairing recently proposed by the weak coupling approaches for the iron oxypnictide superconductors. It indicates that the  $s_{\pm}$ -wave pairing is realized not only in the weak correlation regime but also in the strong correlation regime.

As for the SC II phase, the most dominant pairing is found to be the on-site intra-orbital spin-singlet pairing which is consistent with the ordinary  $s$ -wave pairing of BCS superconductors. However, the superconducting mechanism of this phase is due to the charge fluctuation enhanced by the inter-orbital Coulomb interaction and is different from the ordinary BCS superconductivity due to the electron-phonon interaction. Although the SC II phase seems to be realized only for the unrealistic parameter region in our model, it might be realized for a realistic parameter region in the  $d$ - $p$  model which is more close to the iron oxypnictides.<sup>13,28)</sup> We will address such problem by applying the present method to the  $d$ - $p$  model in the future.

- 1) Y. Kamihara, T. Watanabe, M. Hirano, and H. Hosono: J. Am. Chem. Soc. 130 (2008) 3296.
- 2) Z.-A. Ren, W. Lu, J. Yang, W. Yi, X.-L. Shen, Z.-C. Li, G.-C. Che, X.-L. Dong, L.-L. Sun, F. Zhou, and X.-X. Zhao: Chin. Phys. Lett. 25 (2008) 2215.
- 3) X. H. Chen, T. Wu, G. Wu, R. H. Liu, H. Chen, and D. F. Fang: Nature 453 (2008) 761.
- 4) G. F. Chen, Z. Li, D. Wu, G. Li, W. Z. Hu, J. Dong, P. Zheng, J. L. Luo, and N. L. Wang: Phys. Rev. Lett. 100 (2008) 247002.
- 5) H. Kito, H. Eisaki, and A. Iyo: J. Phys. Soc. Jpn. 77 (2008) 063707.
- 6) D.J. Singh, and M.H. Du: Phys. Rev. Lett. 100 (2008) 237003.
- 7) S. Ishibashi, K. Terakura, and H. Hosono: J. Phys. Soc. Jpn. 77 (2008) 053709.
- 8) K. Nakamura, R. Arita, and M. Imada: J. Phys. Soc. Jpn. 77 (2008) 093711.
- 9) K. Kuroki, S. Onari, R. Arita, H. Usui, Y. Tanaka, H. Kontani, and H. Aoki: Phys. Rev. Lett. 101 (2008) 087004.
- 10) I. I. Mazin, D.J. Singh, M.D. Johannes, and M.H. Du: Phys. Rev. Lett. 101 (2008) 057003.
- 11) F. Wang, H. Zhai, Y. Ran, A. Vishwanath, and D.-H. Lee: Phys. Rev. Lett. 102 (2009) 047005.
- 12) T. Nomura: J. Phys. Soc. Jpn. 78 (2009) 034716; J. Phys. Soc. Jpn. 77 (2008) Suppl. C, 123.
- 13) Y. Yanagi, Y. Yamakawa, and Y. Ōno: J. Phys. Soc. Jpn. 77 (2008) 123701; J. Phys. Soc. Jpn. 77 (2008) Suppl. C, 149.
- 14) H. J. Schulz: Phys. Rev. Lett. 64 (1990) 2831; A. Sudbø, C.M. Varma, T. Giamarchi, E.B. Stechel and T. Scalettar: Phys. Rev. Lett. 70 (1993) 978; M. Ogata, M. U. Luchini, S. Sorella and F. F. Assaad: Phys. Rev. Lett. 66 (1991) 2388.
- 15) K. Sano and Y. Ōno: J. Phys. Soc. Jpn. 72, 1847 (2003), J. Phys.: Condens. Matter 19 (2007) 14528.
- 16) D. G. Shelton and A. M. Tsvelik: Phys. Rev. B53, 14036 (1996).
- 17) S. Q. Shen, Phys. Rev. B57 (1998) 6474.
- 18) H. C. Lee, P. Azaria and E. Boulat: Phys. Rev. B 69 (2004) 155109.
- 19) H. Sakamoto, T. Momoi and K. Kubo: Phys. Rev. B 65 (2002) 224403 .
- 20) T. Shirakawa, Y. Ohta, S. Nishimoto: J. Mag. Mag. Mater. 310 (2) (2007) 663.
- 21) K. Sano and Y. Ōno: J. Mag. Mag. Mater. 310 (2) (2007) e319.
- 22) J. Solyom: Adv. Phys. 28 (1979) 201.
- 23) J. Voit: Rep. Prog. Phys. 58 (1995) 977.

- 24) V. J. Emery: in *Highly Conducting One-Dimensional Solids*, edited by J. T. Devreese, R. Evrand and V. van Doren, (Plenum, New York, 1979) p.327.
- 25) L. Balentz and M.P.A. Fisher: Phys. Rev. **B53** (1996) 12133.
- 26) M. Fabrizio: Phys. Rev. B **54** (1996) 10054.
- 27) V. J. Emery, S. A. Kivelson and O. Zachar: Phys. Rev. **B59** (1999) 15641. A. Leithe-Jasper, W.Schnelle, C. Geibel, and H. Rosner: Phys. Rev. Lett. 101, (2008) 207004.
- 28) K. Sano and Y. Ōno: Physica **C205** (1993) 170; Phys. Rev. **B51** (1995) 1175; Physica **C242** (1995) 113.